Hygrothermal assessment of internally insulated historic solid masonry walls with focus on the thermal bridge due to internal partition walls

Jensen, N. F.; Rode, C.; Møller, E. B.

Published in:
Journal of Physics: Conference Series

DOI (link to publication from Publisher):
10.1088/1742-6596/2069/1/012079

Publication date:
2021

Document Version
Publisher's PDF, also known as Version of record

Hygrothermal assessment of internally insulated historic solid masonry walls with focus on the thermal bridge due to internal partition walls

Hygrothermal assessment of internally insulated historic solid masonry walls with focus on the thermal bridge due to internal partition walls

N F Jensen[1,2,*], C Rode[1] and E B Møller[1]

[1]Technical University of Denmark, Department of Civil Engineering, Brovej, Building 118, 2800 Kgs. Lyngby
[2]Aalborg University, Department of the Built Environement, 2450 Copenhagen, Denmark

Corresponding e-mail: nfj@build.aau.dk

Abstract. This study investigated the hygrothermal performance of five insulation systems for internal retrofitting purposes. Focus was on the hygrothermal performance near partition brick walls compared to the middle of the wall. The setup comprised two insulated reefer containers with controlled indoor climate, reconfigured with several holes containing solid masonry walls with interior embedded wooden elements, an internal brick partition wall and different internal insulation systems, with and without exterior hydrophobisation. Relative humidity and temperature were measured over five years in the masonry/insulation interface and near the interior surface, in the centre of the test field and near the partition wall. In addition, calibrated numerical simulations were performed for further investigation of the thermal bridge effect. Findings for the masonry/insulation interface showed higher temperatures and lower relative humidity near the partition wall in comparison with the central part of the wall. Near the interior surface, measurements showed only minor differences between the two locations. The relative effect of the thermal bridge was smaller in the case of a high driving rain load on the exterior surfaces. The numerical simulations showed that the hygrothermal conditions were affected further away from the partition wall than what could be measured in the experimental setup.

1. Introduction

A high energy saving potential is found in retrofitting historic masonry external walls. Studies of the Danish building stock have shown average-weighted U-values of 2.80 and 0.62 W/(m^2·K) for external walls in multi-story residential buildings built prior to 1850 and in the period 1850-1930, respectively [1]. Many such buildings may have facades that are worth of preservation, which prohibits major exterior alterations, and internal insulation may often be the only option for thermally upgrading the external walls. However, from a building physics point of view, external insulation is preferred as the existing wall is kept warm and protected from the outside climate, while internal insulation is generally regarded as problematic since the reduced heat flow to the existing wall makes the wall become colder [2-3]. This increases the risk of interstitial condensation and moisture-induced damage such as fungal growth, wood decay and frost damage. Another disadvantage is that internal insulation in contrast to external insulation does not solve issues with thermal bridges at the intersections between the external wall and adjoining building elements such as floor partitions and internal partition walls. The thermal bridges represent a significant share of the heat losses through the building envelope and could lead to

local increases in relative humidity (RH) on the interior surfaces due to lower temperatures [4]. Many studies dealing with internal insulation of solid external walls tend not to consider the hygrothermal conditions near thermal bridges. Furthermore, in recent years, strategies for internal insulation have changed away from traditional diffusion-tight systems including a vapour barrier to diffusion-open and capillary active systems. Findings regarding these systems are mixed, with some studies observing good performance [5-7] while other studies suggest better performance of the diffusion-tight systems, if combined with certain additional measures [8-11].

This study investigates the effect of the thermal bridge created by internal partition walls when dealing with internal insulation of solid masonry walls in historic buildings. The study supplements previous investigations of diffusion-open and diffusion-tight internal insulation systems presented in [10-11], which focused on the hygrothermal conditions in the masonry/insulation interface and in the embedded wooden elements and the effects of combining internal insulation with additional measures.

2. Methods and materials

2.1. Experimental setup

A large experimental setup was constructed by the Department of Civil Engineering at the Technical University of Denmark (DTU) on the test site in Kongens Lyngby, Denmark (55.79°N, 12.53°E). The setup comprised several test walls constructed to emulate a section of a Danish historic multi-story building from the period 1850-1930, in relation to both design and materials. The setup consisted of two 40-foot insulated reefer containers with twenty-four 1 x 2 m cut outs made in the façades to accommodate the test walls. Next, twenty-four identical solid masonry walls with the dimensions (HxWxD) 1987 mm by 948 mm by 358 mm (1½ stones thick with 10 mm interior rendering) were constructed in the cut outs (Figure 1). As shown in the figure, the test walls were constructed as a 3-dimensional set-up, which included a wooden internal floor construction (with a wooden beam end embedded 100 mm into the masonry wall, supported by a wooden wall plate, blue arrows in Figure 1) and a 108 mm (½-stone) internal partition wall made of masonry with render on both sides (red arrows in Figure 1). Special care was made to reduce potential sources of error from unintentional heat, air or moisture transport, additional information about the measures are available in [10, 12].

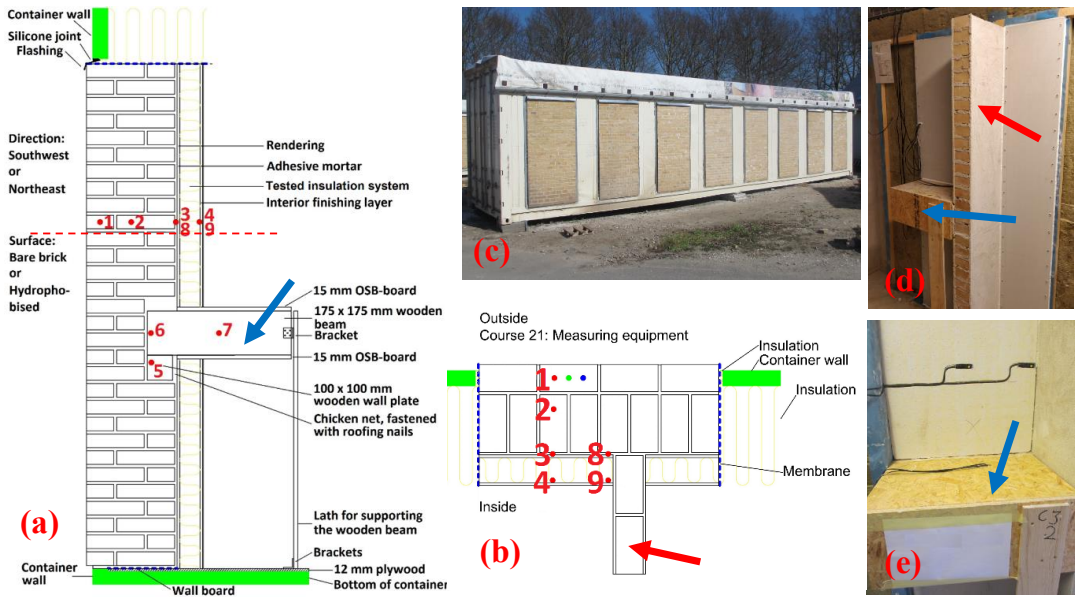

Figure 1. Test stand configuration: (a) Vertical section of a test wall; (b) Horizontal section of a test wall through the 21st brick course, showing sensor locations (shown with a red dashed line in Figure 1a); (c) External view of one of the test containers; (d) Internal view of a test wall including partition wall and floor construction, (e) Sensor installation near the interior surface in a test wall, mid and near partition wall. Red dots show sensor locations.

Thirteen of the twenty-four test walls are presented in this paper and the five applied insulation systems are listed below. The properties of the individual materials are listed in Table 1.

1) **MW (1 wall)**: 100 mm mineral wool, polyethylene vapour barrier, and 13 mm gypsum board.
2) **Phenolic foam (4 walls)**: 5 mm glue mortar, perforated aluminium foil, 100 mm phenolic foam, aluminium foil barrier, and 13 mm gypsum board.
3) **PUR-CS (4 walls)**: 10 mm glue mortar, 80 mm polyurethane foam with calcium silicate channels, 10 mm render, and 3 mm surface filler.
4) **CaSi (2 walls)**: 10 mm glue mortar, 100 mm calcium silicate, and 8 mm render.
5) **AAC (2 walls)**: 8 mm glue mortar, 100 mm autoclaved aerated concrete, and 8 mm render.

Five walls were examined with and without exterior silane/siloxane-based hydrophobisation: two with phenolic foam, two with PUR-CS and one with AAC. Note that exterior hydrophobisation is abbreviated as "+H" in the results section. The influence of Wind Driving Rain (WDR) and high/low solar irradiation was assessed by orienting eight of the thirteen test walls South-West (prevailing direction for WDR in Denmark, SW, 237°) and five towards North-East (NE, 57°). The five walls facing North-East were: two with phenolic foam (with and without hydrophobisation), two with PUR-CS (with and without hydrophobisation) and one with CaSi. The phenolic foam system was installed 2½ years after initial project start (in Nov. 2017) on test walls previously fitted with a non-commercial system.

Table 1. Materials and their hygrothermal properties.

Materials	Density, ρ [kg/m^3]	Thermal conductivity, λ_{dry} [W/(m·K)]	Water vapour resistance factor, μ_{dry} [-]	Water absorption coefficient, A_w [kg/(m^2·s^{½})]
Yellow masonry brick	1643	0.600	16.9	0.278
7.7% lime mortar render	1243	0.440	22.4	0.390
Mineral wool	37	0.040	1	0
Phenolic foam	35	0.020	114	0.009
PUR-CS foam	49	0.037	27.01	0.013
Calcium silicate	225	0.061	4.23	0.726
Autoclaved aerated concrete	99	0.044	3	0.006

Materials were characterised by Technische Universität Dresden within the RIBuild project. Properties of the remaining materials are available in the supplementary files [12].

Temperature and RH were measured and logged every 10 minutes in the sensor locations shown in Figure 1a-b. Focus was on sensors in the masonry/insulation interface and near the interior surface in Figure 1b, abbreviated as P3, P4, P8 and P9. The distance between sensors P3/P4 and P8/P9 was 220 mm. For detailed sensor information, please see [12]. The indoor environment was conditioned to 20 °C and 60% RH throughout the whole measuring period (May 1st 2015 to May 1st 2020), no cooling or dehumidification was used, and temperature and RH could therefore exceed this level in summer.

2.2. Calibrated numerical simulations

The numerical simulations were carried out to study how the thermal bridge created by the internal partition wall affects the hygrothermal conditions in the test walls of the experimental setup. The simulations were performed using the Delphin 6 software and the wall models were simulated for 5-years for five test walls facing south-west: PUR-CS with/without hydrophobisation, AAC with/without hydrophobisation, and CaSi. The 2D models were created as shown in Figure 1b with the above-mentioned layers and thicknesses for the individual insulation systems, including the mortar joints. The models were calibrated against measured RH and temperature data for sensors 1-4 and 8-9, using measured initial conditions and interior/exterior boundary conditions from the experimental setup. Exterior hydrophobisation was simulated by reducing the water uptake coefficient, A_w, by a factor 1000 for the outermost 10 mm of the masonry wall. The boundary coefficients were set as follows: Ground reflection (albedo) 0.25 [-], Short wave absorption 0.7 [-], Long wave emission 0.9 [-], Rain exposure

coefficient 0.7-1.0 [-], Internal/external heat exchange coefficient 5.0/13.2 [W/(m^2·K)], Internal/ external vapour exchange coefficient $3.0 \cdot 10^{-8}/2.0 \cdot 10^{-7}$ [s/m].

2.3. Assessing the risk of fungal growth

The widely used VTT mould-growth model by Hukka and Viitanen [13] was applied to produce a theoretical prediction of the risk of fungal growth. Model output is the mould index (M), ranging from 0 to 6, where 0 corresponds to no growth and 6 to heavy growth (100% coverage). Values 3-6 are fungal growth within the visual range. For systems using adhesive mortar the growth predictions in the masonry/insulation interface were started after one year (on 01-05-2016) to emulate the effect of the alkaline conditions during the initial dry out, as proposed in [10-11, 14].

3. Results and discussion

3.1. Hygrothermal measurements for walls without exterior hydrophobisation

A comparison between the temperature measurements in P3 and P8 in the masonry/insulation interface is shown in Figure 2 and three tendencies were observed. 1) P3 was generally 0.5-1°C warmer than P8 in walls facing south-west during summer periods; 2) P3 was generally 0.5-1°C colder than P8 in walls facing north-east during summer periods; 3) P3 was 2-4 °C colder than P8 during winter periods, no differences were observed between orientations. The observed differences between orientations during summer were probably caused by the higher solar radiation from South-West and that the heat flow from the outside could easier penetrate to the inside through the thermal bridge due to the lower thermal resistance in comparison with the middle of the test wall (P3). This resulted in lower temperatures in P8 in walls facing south-west. The higher temperatures observed in P8 during winter periods were due to the higher heat flow passing through the thermal bridge.

For the interior surface, two tendencies were observed from the comparison between temperatures in P4 and P9. 1) P4 was 0.5-1°C colder than P9 during summer. 2) P4 was 1-2 °C warmer than P9 during winter. No considerable differences were observed between orientations in terms of temperature near the interior surface, as would be expected since these locations would be affected primarily by the indoor climate rather than the outdoor. It was also observed that the applied insulation systems generally experienced relatively similar temperatures and trends near the interior surface, with the exception of the unhydrophobised wall with Phenolic foam facing South-West, which in contrast to the other test walls experienced higher temperatures in P9 by 1.5-2 °C (see supplementary files [12]). However, it was discovered that this was caused by unintentional heating of near the partition wall by the exhaust fan of the logging computer. This was found to have affected the RH levels near the interior surface.

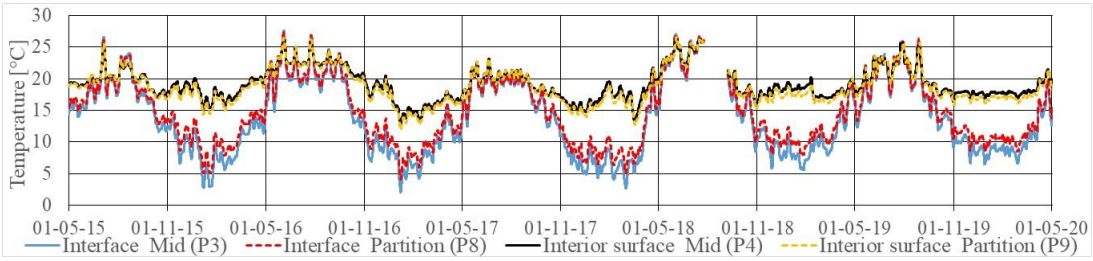

Figure 2. General representation of the temperatures in the middle of the test wall and near the internal partition wall in the masonry/insulation interface and interior surface. Shown for the CaSi_SW test wall.

In terms of RH levels in the masonry/insulation interface, it was observed that the larger heat flow through the thermal bridge and the higher temperatures in P3 had little or no effect on the RH levels in the unhydrophobised test walls facing South-West (red and blue lines in Figure 3a-b). This suggests that the high WDR load from South-West cancelled out the potential reduction in the RH levels which would have occurred due to the higher temperatures. For the unhydrophobised test walls facing North-East

with lower WDR load, the RH levels were generally lower in comparison with the walls facing South-West and the larger heat flow through the thermal bridge was generally seen to lower the RH levels in P8 in the masonry/insulation interface all year round by up 10-20%-points in comparison with P3 (red and blue lines in Figure 3c). In addition, it was seen that the drop in RH levels occurring in the interface during summer periods in walls with highly diffusion-open systems (CaSi and AAC) facing south-west extended further into the autumn in the areas in P8 in comparison with P3 due to the increased heat flow (Figure 3b).

For the interior surface, it was seen that there were different trends for the diffusion-tight systems and for the highly diffusion-open (Figure 3a-b). As reported in [10], the RH levels near the interior surface in the highly diffusion-open systems followed the RH levels in the indoor air with a slightly addition of a few %-point RH. However, a completely different picture was seen for the diffusion-tight systems with low RH levels in winter and near 100% RH in summer, suggesting that the vapour barrier was correctly installed. The high RH levels during summer was due to summer condensation on the cold side of the vapour barrier. In terms of differences between P4 and P9, rather limited differences were seen for the highly diffusion-open systems, with only slightly higher RH levels in P9 (Figure 3b). For the diffusion-tight systems, larger differences were observed between P4 and P9 near the interior surface during the winter periods, where the RH levels in P9 were 8-12%-point higher in comparison with P3 as a result of the lower temperatures (Figure 3a).

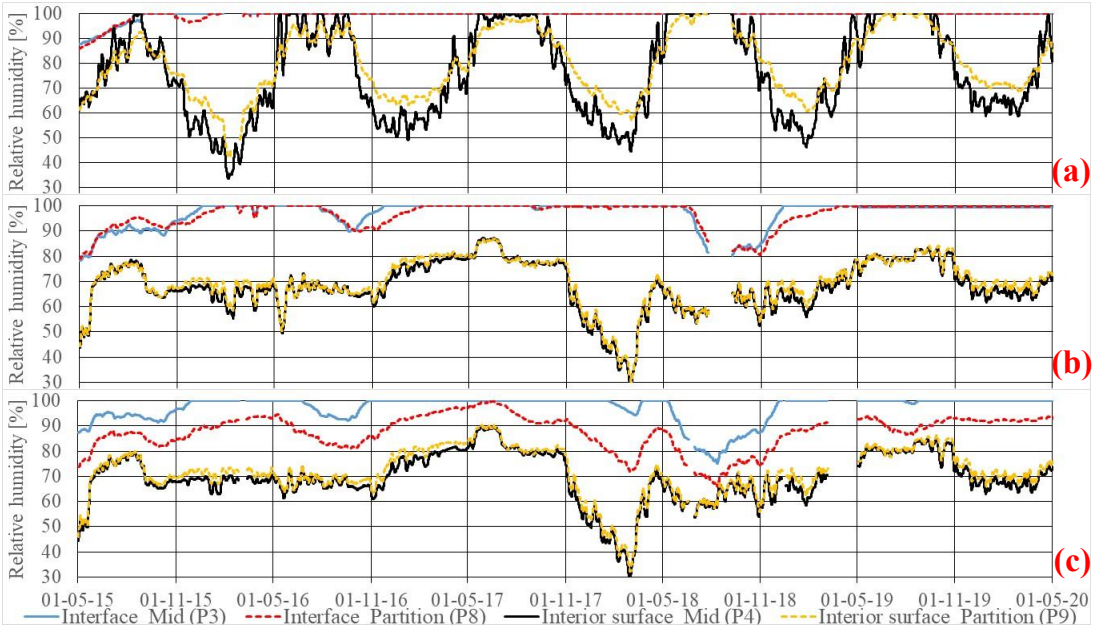

Figure 3. General representation of the RH levels in the middle of the test wall and near the internal partition wall in the masonry/insulation interface and interior surface in walls without hydrophobisation: (a) diffusion-tight systems facing South-West, shown with MW_SW; (b) diffusion-open systems facing South-West, shown with CaSi_SW; (c) trends for walls facings North-East, shown with CaSi_NE. The drop in RH in early 2018 was due to a faulty humidifier.

3.2. Hygrothermal measurements for walls with exterior hydrophobisation

With reduced WDR intrusion due to exterior hydrophobisation, it was observed that the larger heat flow through the thermal bridge led to lower RH levels in the masonry/insulation interface in P8 (Figure 4). This is similar to the trends seen for the unhydrophobised walls facing North-East, with a low WDR load. The effect of the thermal bridge on the RH levels in the masonry/insulation interface was seen to differ between the more diffusion-tight systems (Figure 4a-b) and the highly diffusion-open non-

capillary active AAC (Figure 4c). Larger differences in RH levels were observed between the middle of the test wall vs near the partition wall with the AAC system compared with the more diffusion-tight systems. This was probably related to the poor combination of exterior hydrophobisation with a highly diffusion-open system as documented in [10-11]. While the hydrophobisation does successfully prevent rain intrusion, the highly diffusion-open nature of the AAC allows more outward moisture diffusion from the indoor environment during winter compared with the more diffusion-tight systems, resulting in more interstitial condensation in the AAC wall. Furthermore, the lack of good capillary transporting properties means that the AAC is not able to effectively move the moisture away from the masonry/insulation interface. However, in P8, the higher heat flow seems to balance out the increase in RH from the outward moisture diffusion, resulting in RH levels that were generally below 90%. This suggests that when applying highly diffusion-open non-capillary insulation, a smaller insulation thickness is preferable. Lastly, a comparison between the systems during the period with faulty humidifier (Nov. 2017 – Feb. 2018) and rapidly decreasing RH levels, showed that P8 in the masonry/insulation interface responded faster than P3. This was seen not only for the highly diffusion-open systems but also for the more diffusion-tight (Figure 3c and Figure 4a-b).

Near the interior surface, the differences in RH levels between P4 and P9 were observed to be slightly larger than seen for the unhydrophobised walls.

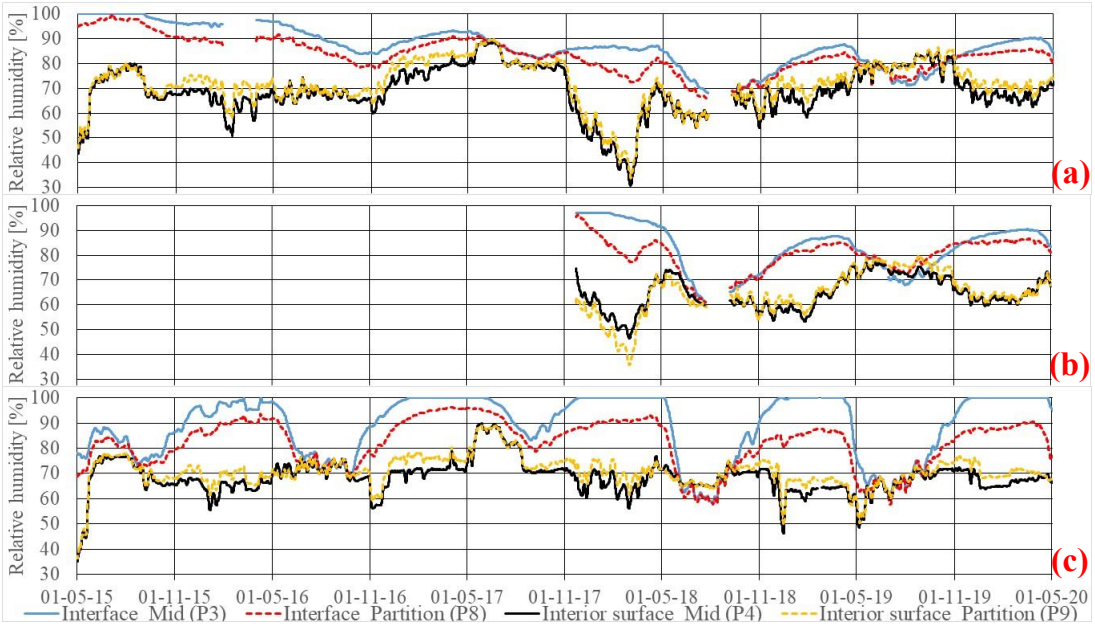

Figure 4. *RH in the middle of the test wall and near the internal partition wall in the masonry/insulation interface and interior surface in walls with hydrophobisation: (a) PUR-CS+H_SW; (b) Phenolic+H_SW; (c) AAC+H_SW.*

3.3. Risk of fungal growth

For the masonry/insulation interface, it was observed that the VTT mould index was higher in the middle of the wall (P3) compared with near the partition wall (P8) (Table 2). This shows that the higher temperatures and lower RH levels near the partition wall due to the increased heat flow reduced the risk of fungal growth. Near the interior surface, there was no clear indication of where the VTT mould index would be highest; the slightly lower temperatures near the internal partition wall (P9), and the associated increase in the RH levels resulted in little or no difference in relation to the risk of fungal growth in comparison with the middle of the test wall (P4). Furthermore, the mould index in P4 and P9 was low in all cases except for the MW system.

Table 2. Max VTT mould index [-] in the masonry/insulation interface and near the interior surface.

System type	Semi diffusion-tight				Highly diffusion-tight					Highly diffusion-open			
Measurement location	PUR-CS+H (SW)	PUR-SM (SW)	PUR-CS+H (NE)	PUR-CS (NE)	MW (SW)	Phenolic+H (SW)	Phenolic (SW)	Phenolic+H (NE)	Phenolic (NE)	CaSi (SW)	CaSi (NE)	AAC (SW)	AAC+H (SW)
Interface, mid (P3)	0.57	3.50	3.50	3.49	5.30	0.44	3.39	3.46	3.12	3.50	3.50	3.50	3.50
Interface, wall (P8)	0.26	3.50	2.70	1.13	5.30	0.10	3.50	1.60	1.85	3.45	1.57	3.50	2.87
Int. Surf., mid (P4)	0.07	0.05	0.10	0.05	5.30	0.00	0.31	0.00	0.00	0.03	0.09	1.30	0.71
Int. Surf., wall (P9)	0.08	0.03	0.13	0.08	5.30	0.00	0.00	0.00	0.00	0.02	0.10	1.00	0.68

Yellow highlights show the highest M-values between middle of the wall and near the internal partition wall. For comparison, the M-values for the interior surface of uninsulated reference walls (mid/partition wall) were: Ref1_SW 0.49/0.73; Ref2_NE 0.41/0.79; Ref3_SW 0.10/0.09. The measurements are available in [12].

3.4. Numerical simulations

The simulated RH and temperature profiles (Figure 5) show that the higher heat flow from the thermal bridge affected RH and temperature throughout the entirety of the test wall shown in Figure 1b and could therefore have affected the measurements in sensor location P3 for the masonry/insulation interface. Results from the wall models with extended width (see supplementary files [12]) suggest that the temperatures and RH levels in the masonry/insulation interface were affected up to a distance of 1.0-1.2 m from the thermal bridge. It was observed that the temperatures in P8 were 4-5°C higher than seen for the masonry/insulation interface in areas unaffected by the thermal bridge (similar to P3 but further away from the thermal bridge) during the coldest winter periods. For the RH levels in the interface, the differences between P8 and areas unaffected by the thermal bridge were typically within 3-5% RH. Larger differences of 8-12% RH were in periods observed between P8 and the unaffected areas in wall models with exterior hydrophobisation. In addition, a comparison between the CaSi, AAC and PUR-CS systems suggests that with increasing thermal resistance of the insulation system, the effects of the thermal bridge through the partition wall reaches further inwards into the building. This is probably due to the masonry wall being warmer in the test walls with the less insulating systems, which decreased the thermal bridge effect of the partition wall.

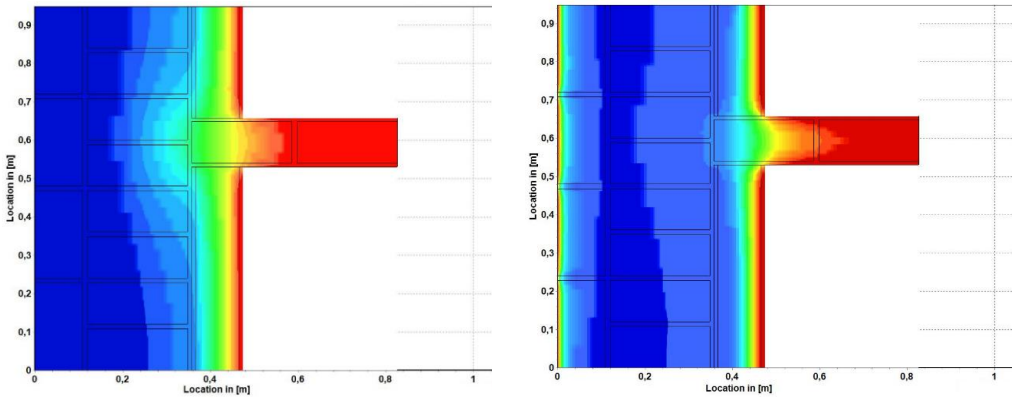

Figure 5. Simulated horizontal section through the 21st brick course in the AAC_SW wall model on March 1st 2018: (a) Temperature profile, goes from blue T ≤ 0 °C to red T ≥ 20 °C; and (b) RH profile, goes from red RH ≤ 50% to blue RH = 100%.

4. Conclusion

This study investigated the effect of the thermal bridge created by internal partition walls when dealing with internal insulation of solid masonry walls in historic buildings. The effect of exterior hydrophobisation was also investigated. It was shown that the higher heat flow near the partition wall resulted in less critical temperatures and RH conditions in the masonry/insulation interface, while it was found that the effect on the temperatures and RH conditions near the interior surface were rather limited with slightly aggravated moisture conditions in some test walls. Furthermore, it was found that the WDR load had a large impact on the hygrothermal conditions. It was found that in the case of low WDR load, either due to the orientation or due to exterior hydrophobisation, the relative effect of the thermal bridge increased leading to larger differences between the middle of the test wall (P3 and P4 in Figure 1) and places near the partition wall (P8 and P9 in Figure 1) compared with test walls with high WDR load.

In terms of the risk of fungal growth, it was shown with the theoretical predictions that the thermal bridge reduced the risk in the masonry/insulation interface near the partition wall (P8) compared with areas, which were near the middle of the test walls (P3), while no considerable difference was seen near the interior surface (P4 and P9). In addition, the predictions indicate that the hygrothermal conditions seen for the semi/highly diffusion-tight insulation systems in combination with exterior hydrophobisation do not support fungal growth, neither in the middle of the test walls nor near the thermal bridge. In contrast, it was found that test walls without hydrophobisation or highly diffusion-open systems with hydrophobisation could lead to fungal growth in the masonry/insulation interface, but that the conditions were slightly better near the thermal bridge. Based on the numerical simulations, it was found that the higher heat flow through thermal bridge affected the hygrothermal conditions in the exterior solid masonry test walls as far as 1.0-1.2 m away from the internal partition wall. It was also found that the effects of the thermal bridge through the partition wall reached further inwards into the buildings with increasing thermal resistance of the insulation system.

This research was financially supported by the European Union's Horizon 2020 research and innovation program under grant agreement No 637268 – as part of the RIBuild project; and by the Landowners Investment Foundation (Grundejernes Investeringsfond).

References

[1] Kragh J and Wittchen K B 2014 *Energy Build.* **68** p 79–86
[2] Straube J and Schumacher C 2007 *J. Green Build.* **2** no. 2 p 42–50
[3] Gorse C and Highfield D 2009 *Refurbishment and Upgrading of Buildings, second ed.* (Taylor & Francis, New York, USA)
[4] Sallée H, Quenard D, Valenti E and Galan M 2014 *Energy Build.* **85** p 631-37
[5] Odgaard T, Bjarløv S P and Rode C 2018 *Build. Environ.* **129** p 1–14
[6] Morelli M and Møller E B 2019 *Sci Technol Built Environ* **25** no. 9 p 1199–1211
[7] De Mets T, Tilmans A and Loncour X 2017 *Energy Procedia* **132** p 753–58
[8] Klõšeiko P, Arumägi E and Kalamees T 2015 *J. Build. Phys.* **38** no. 5 p 444–64
[9] Hansen T K, Bjarløv S P, Peuhkuri R H and Harrestrup M 2018 *Energy Build.* **172** p 235–48
[10] Jensen N F, Odgaard T R, Bjarløv S P, Andersen B, Rode C and Møller E B, 2020 *Build. Environ.* **182** 107011
[11] Jensen N F, Bjarløv S P, Rode C, Andersen B and Møller E B 2021 *J. Build. Phys. Postprint* DOI: 10.1177/1744259120988745
[12] Jensen N F, Rode C and Møller E B 2021 Dataset DOI: 10.11583/DTU.13739593
[13] Ojanen T, Viitanen H, Peuhkuri R, Lähdesmäki K, Vinha J and Salminen K 2010 Proc. – Thermal Performance of the Exterior Envelopes of Whole Buildings : Buildings XI
[14] Viitanen H, Krus M, Ojanen T, Eitner V and Zirkelbach D 2015 *Energy Procedia* **78** p 1425-30